A Comparison of Retinal Morphology Viewed by Optical Coherence Tomography and by Light Microscopy

Cynthia A. Toth, MD; Drew G. Narayan; Stephen A. Boppart, MSEE; Michael R. Hee, MSEE; Jim G. Fujimoto, PhD; Reginald Birngruber, PhD; Clarence P. Cain, PhD; Cheryl D. DiCarlo, DVM; W. Patrick Roach, PhD

Objective: To compare the cross-sectional images of primate retinal morphology obtained by optical coherence tomography (OCT) with light microscopy to determine the retinal components represented in OCT images.

Methods: Laser pulses were delivered to the retina to create small marker lesions in a *Macaca mulatta*. These lesions were used to align in vivo OCT scans and ex vivum histologic cross sections for image comparison.

Results: The OCT images demonstrated reproducible patterns of retinal morphology that corresponded to the location of retinal layers seen on light microscopic overlays. Layers of relative high reflectivity corresponded to horizontally aligned retinal components such as the nerve fiber layer and plexiform layers, as well as to the retinal pigment epithelium and choroid. In contrast, the nuclear layers and the photoreceptor inner and outer segments demonstrated relative low reflectivity by OCT.

Conclusions: Retinal morphology and macular OCT imaging correlate well, with alignment of areas of high and low reflectivity to specific retinal and choroidal elements. Resolution of retinal structures by OCT depends on the contrast in relative reflectivity of adjacent structures. Use of this tool will enable expanded study of retinal morphology, both normal and pathologic, as it evolves in vivo.

Arch Ophthalmol. 1997;115:1425-1428

From Duke University Eye Center, Durham, NC (Dr Toth and Mr Narayan); Massachusetts Institute of Technology, Cambridge (Messrs Boppart and Hee and Dr Fujimoto); Medizinisches Laserzentrum, Lübeck, Germany (Dr Birngruber); TASC Inc, San Antonio, Tex (Dr Cain); Uniformed Services University of the Health Sciences, Bethesda, Md (Dr DiCarlo); and Air Force Office of Scientific Research, Bolling AFB, Washington, DC (Dr Roach).

LIGHT MICROSCOPY has been a gold standard for analysis of retinal morphology at the micron to millimeter scale. There has historically been no in vivo tool capable of resolving the small structures that comprise the retinal layers. Traditional ophthalmic ultrasound is limited to resolution of 75 µm. Scanning laser ophthalmoscopy, although using visible and infrared radiation for in vivo imaging, does not display a vertical cross section of structures within the retina.[1-3] Numerous new optical ranging systems have been proposed to delineate the structure of normal retina and of disease processes within its tissues. Optical coherence tomography (OCT) is one of these techniques, and has been applied in numerous studies of healthy and diseased human tissues,[3-9] although without clinicopathologic correlation. In this study, we provide a direct comparison of OCT and histologic images of the *Macaca mulatta* macula.

RESULTS

The OCT images demonstrated clear reproducible patterns of retinal structure. From scan to scan, the overall level of retinal reflectivity varied, possibly because of small variations in corneal hydration and alignment of the scanning beam with respect to the retina. The relative reflectivity of retinal layers did not vary, ie, the retinal components always maintained the same relationship of RHR or RLR as described below.

The retinal thickness measured from the histologic section was greater than the OCT image in both eyes. The histologic images averaged 4% and 12% larger than the corresponding OCT image in the right and left eye, respectively.

A layer of RHR corresponded to the location of the nerve fiber layer (solid arrow in Figure 3, left). Although this signal varied in intensity, the nerve fiber layer was the most highly reflective of all neurosensory retinal layers, matching or exceeding the underlying plexiform layers. The depth of the region of RHR corresponded to the thickness of the nerve fiber layer by light microscopy. Thus, the RHR layer increased in thickness with increasing proximity to the optic nerve.

Additional layers of RHR corresponded to the location of the plexiform

MATERIALS AND METHODS

A mature *M mulatta* was maintained under standard laboratory conditions in accordance with the Association of Vision Research in Ophthalmology Statement for the Use of Animals in Ophthalmic and Vision Research and federal guidelines.

Preoperative care, anesthesia, intraoperative and postoperative care, euthanasia, and tissue processing were performed as previously published.[10] Animals were anesthetized during all procedures including laser lesion placement and OCT scanning and image acquisition. In this study, we used 5-picosecond, 580-nm, 0.02- to 0.10-mJ laser pulses to create retinal lesions, rather than the argon laser as previously reported.[9] The refractive error for the 2 eyes was +0.50 −0.25 ×180 OD and +0.25 OS. The OCT imaging was not scaled for the minimal refractive error.

To correlate histologic sections with OCT images, the retinal laser lesions were observed through the fundus camera, allowing alignment of the OCT imaging beam over the center of each lesion. The margins of the laser lesions were used to align the overlay of OCT and light micrograph cross sections.

The OCT scan, a 2-dimensional cross-sectional high-resolution retinal image, was acquired in 4 seconds by assembling 200 adjacent longitudinal (depth) profiles of optical backscattered intensity as the OCT imaging beam was scanned across 500 μm of retina (200×250 pixels). For OCT, the color spectrum depicting the logarithmic scale of reflectivity (left parts of **Figure 1**, **Figure 2**, and **Figure 3**) is arbitrary with the red end of the spectrum selected for pixels corresponding to sites of relative high reflectivity (RHR) (backscatter), and blue for relative low reflectivity (RLR).

For each site, OCT scans were obtained immediately before and after laser placement. The retina adjacent to the laser lesion, but greater than 100 μm from the margins of the laser lesion, was used for comparison (Figure 1).

The macula was oriented for sectioning in the plane of OCT scans. Digital images of sections and a micrometer were obtained using a Zeiss light microscope with a charge coupled diode (CCD) camera feeding to a personal computer (Macintosh, Apple, Cupertino, Calif). Images were captured using Scion Image (National Institutes of Health program, Bethesda, Md) and stored and manipulated using Adobe Photoshop (Adobe Systems Inc, Mountain View, Calif). The distance between the nerve fiber layer and the retinal pigment epithelium (RPE) was measured with the micrometer image at 4 or more sites on the light micrographs. The OCT images were measured at corresponding locations using the 250-μm scale bar. Correction for the difference between image size was achieved by compressing the light micrographs equally along both axes, after which the margins of the anatomic layers were traced over the light micrographs and superimposed on the OCT images (Figure 2).

layers of the retina. Throughout the macula, highly reflective regions correspond to areas of horizontal retinal elements, whether nerve fiber layer at the retinal surface or deeper plexiform layers. These layers converged into a single RHR layer over a single layer of RLR in the fovea (Figure 2).

Retinal areas of RLR corresponded to the location of the nuclear layers and the photoreceptor inner and outer segments. The RLR of the outer nuclear layer, and the photoreceptor inner and outer segments together, consistently demonstrated the most prominent broad band of RLR (open arrows in Figures 1 through 3). These vertically aligned structures were the only nonnuclear retinal elements to demonstrate RLR. In the fovea, we also saw convergence of the RLR layers with only a single outer band of RLR present in the center of the fovea.

The choroid and RPE together matched to a wide band of RHR that eventually decreased at greater choroidal depth. In OCT, we could not identify a separate RPE image from the underlying choroid. The RHR of these layers was pronounced and often greater than the reflectivity of the surface nerve fiber layer, despite the fact that this portion of the OCT image traveled through the neurosensory retina twice before detection.

COMMENT

We demonstrated the effectiveness of in vivo OCT in delineating the location and relative reflectivity of elements of the primate macula in cross section in direct correlation to light micrographs of these retinal sites. We also demonstrated some of the limits in the resolution of this OCT system when compared with light microscopic study of fixed, stained tissue. We further showed that imaging retinal structures depended not only on the resolving power of the instrument, but also on the contrast in relative reflectivity of adjacent retinal structures.

Optical coherence tomography and light microscopy are fundamentally different techniques that generate images of microscopic tissue elements. Optical coherence tomography utilizes propagation of light through, and the time delay of light reflected back from, unstained tissue to identify location and relative reflectivity of microstructures. Sites of RHR and RLR correlate with the location of varying backscatter of photons that return to the OCT device for comparison within the coherence length of the source. Images obtained with OCT are thus highly dependent on the optical properties of the structure and cannot be interpreted in the same manner as staining of cellular elements in fixed tissue sections. Thus, the direct histologic correlation in this study helps define the location and types of tissue elements that create variations in optical backscatter and, hence, variations within the OCT image.[2-6]

Light micrographs of fixed tissue, although the gold standard in this comparison, have their own drawbacks. To obtain macular specimens the tissue must be surgically removed, rapidly fixed, and then dehydrated with minimal distortion. The tissue must be embedded with the correct orientation, blocks must be sectioned, and the tissue of interest stained. Visualizing retinal structure depends on the tissue staining or labeling characteristics. Each step adds potential artifact to the final imaging of retinal morphology. Retinal excision is also not an option in most macular evaluation.

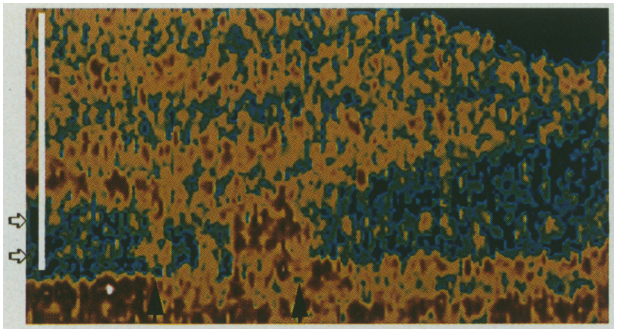

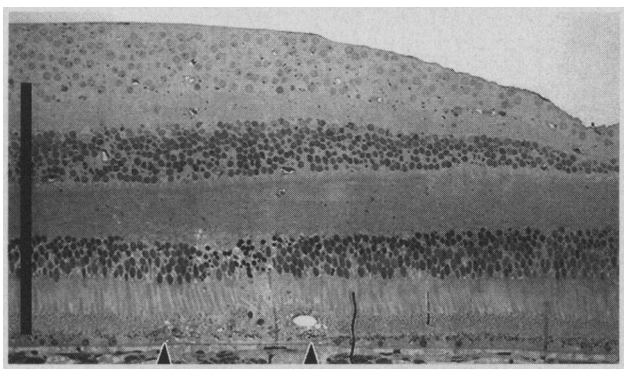

Figure 1. *Optical coherence tomography (OCT) of a section of retina (top) and its corresponding histologic section stained with methylene blue (bottom). Note the laser lesion (created with an estimated retinal spot size of 200 µm) visible in both images (between solid arrowheads). The laser lesion images were aligned for the comparison of adjacent retinal layers as seen in Figure 2. The 250-µm scale bar holds for both the x- and y-coordinates of the OCT image. The open arrows indicate the broad layer of relative low reflectivity corresponding to the photoreceptor nuclei and inner and outer segments.*

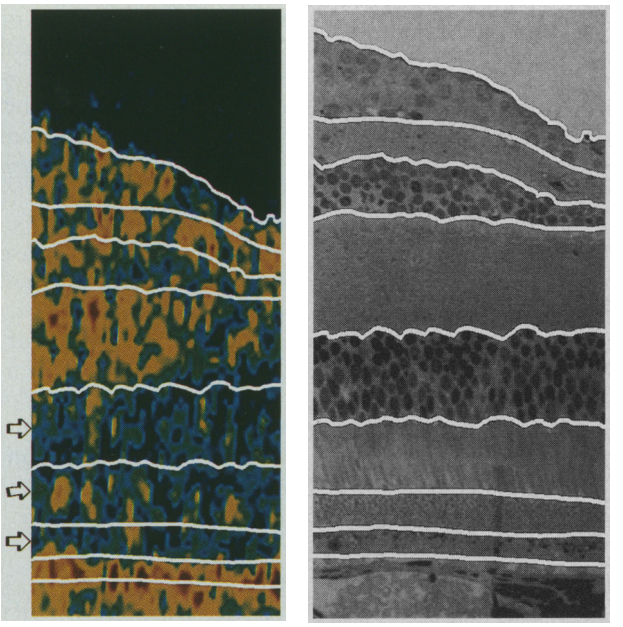

Figure 2. *Optical coherence tomography (OCT) of the macula (left) and its corresponding histologic section stained with methylene blue (right). An outline of the retinal layers from the corresponding light micrograph is superimposed over the OCT image. Note the coalescence of layers entering the fovea. The open arrows indicate the broad layer of relative low reflectivity that corresponds to the nuclear layer and inner and outer segments of the photoreceptors. This layer widens in the fovea.*

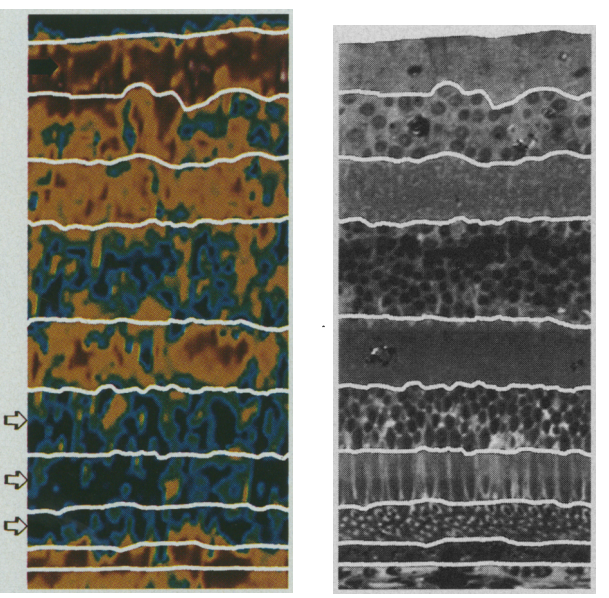

Figure 3. *Optical coherence tomography (OCT) of a section of macula adjacent to another laser lesion (left) and its corresponding histologic section stained with methylene blue (right). An outline of the retinal layers from the corresponding light micrograph is superimposed over the OCT image. This site is further from the fovea than that in Figure 2. As in Figures 1 and 2, the open arrows point to the confluence of relative low reflectivity corresponding to the nuclear layer and inner and outer segments of the photoreceptors.*

In contrast, this OCT system has poorer resolution than light microscopy, and cannot separate the image of adjacent tissues if they have matching relative reflectivity (eg, the RPE and choroid, or photoreceptor outer segments and photoreceptor nuclei). Optical coherence tomography does, however, present an in vivo undisturbed image of retinal structure in situ. The drawbacks of OCT imaging include image processing algorithms that may misrepresent retina surface contours, refractive index effects, and optical attenuation with depth in some tissues or materials. These limitations explain the difficulty in acquiring peripheral retinal images, the dependency of OCT imaging on clear ocular media and a smooth cornea, and the limited axial depth of the OCT image within the choroid (Figures 1 through 3). If OCT measurements are performed in a consistent manner, these effects are a constant part of the baseline. Thus, the diagnostic power of OCT requires that the user understands the method of image acquisition, bases clinical measurements on known correlation with histopathologic characteristics, and relies on detecting deviations from a known baseline.

We have not determined why a particular retinal structure demonstrates RHR or RLR. We hypothesize that it is the horizontal orientation, size, and structure of the nerve fibers and plexiform layer components that determines the RHR. The RHR may also be accentuated in the inner retina where the first major fundus reflection occurs. In contrast, photoreceptor inner and outer segments demonstrate RLR possibly because of their regularly aligned microstructural elements and vertical macrostructure. Intracellular and extracellular fluid, membrane orientation, or a cellular chromophore could also

affect local approximately 840-nm photon absorption or reflectivity, and thus the OCT image. A change in local retinal physiology might be identified only in OCT scans or only in light micrographs or with both techniques. This would depend on whether in vivo reflectivity or ex vivum staining or labeling of tissue elements was affected by the injury or disease process. Further OCT studies and the use of different scanning wavelengths may clarify this.

We recognize that OCT and light microscopy use very different approaches to analyze cellular elements and therefore the images do not describe the same tissue characteristics. However, in this study we have shown a correlation between primate macular structure and of macular OCT images, with close alignment between zones of RHR or RLR and specific retinal or choroidal elements. In future applications, sequential OCT imaging will improve our understanding of the temporal evolution of the morphology of the normal, diseased, or injured retina.

Accepted for publication June 9, 1997.

This research was sponsored by US Air Force (USAF) Armstrong Laboratory, and the Air Force Office of Scientific Research, Air Force Systems Command, under grants F49620-95-1-0226 and 2312AA-92AL014 and contract F33615-92-C-0017. The US Government is authorized to reproduce and distribute reprints for governmental purposes not withstanding any copyright notation thereon.

The views and conclusions contained in this article are those of the authors and should not be interpreted as necessarily representing the official policies or endorsements, either express or implied, of the Air Force Office of Scientific Research or the Government.

We would like to thank Ewa Worniallo for her support of the histopathology effort in preparation of the manuscript.

Reprints: Cynthia A. Toth, MD, Duke University Eye Center, Box 3802, Erwin Road, Durham, NC 27710 (e-mail: toth0004@mc.duke.edu).

REFERENCES

1. Menezes AV, Giunta M, Chisholm L, Harvey PT, Tuli R, Devenyi AG. Reproducibility of topographic measurements of the macula with a scanning laser ophthalmoscope. *Ophthalmology.* 1995;102:230-235.
2. Manivannan A, Kirkpatrick JNP, Sharp PF, Forrester JV. Clinical investigation of an infrared digital scanning laser ophthalmoscope. *Br J Ophthalmol.* 1994;78:84-90.
3. Fujimoto JG, Brezinski ME, Tearney GJ, et al. Optical biopsy and imaging using optical coherence tomography. *Nature Med.* 1995;1:970-972.
4. Hee MR, Puliafito CA, Wong C, et al. Optical coherence tomography of macular holes. *Ophthalmology.* 1995;102:748-756.
5. Hee MR, Izatt JA, Swanson EA, et al. Optical coherence tomography of the human retina. *Arch Ophthalmol.* 1995;113:325-332.
6. Hee MR, Puliafito CA, Wong C, et al. Quantitative assessment of macular edema with optical coherence tomography. *Arch Ophthalmol.* 1995;113:1019-1029.
7. Huang D, Swanson EA, Lin CP, et al. Optical coherence tomography. *Science.* 1991;254:1178-1181.
8. Puliafito CA, Hee MR, Lin CP, et al. Imaging of macular diseases with optical coherence tomography. *Ophthalmology.* 1995;102:217-229.
9. Puliafito CA, Hee MR, Schulman JS, Fujimoto JG. *Optical Coherence Tomography of Ocular Diseases.* Thorofare, NJ: Slack Inc; 1996.
10. Toth CA, Birngruber R, Boppart SA, et al. Retinal argon laser lesions evaluated in vivo by optical coherence tomography. *Am J Ophthalmol.* 1997;123:188-198.